EARTH SURFACE PROCESSES AND LANDFORMS
*Earth Surf. Process. Landforms* **44**, 2437–2449 (2019)
© 2019 John Wiley & Sons, Ltd.
Published online 9 July 2019 in Wiley Online Library
(wileyonlinelibrary.com) DOI: 10.1002/esp.4673

Check for updates

# Flow resistance and hydraulic geometry in bedrock rivers with multiple roughness length scales

**Robert I. Ferguson,* Richard J. Hardy and Rebecca A. Hodge**
Department of Geography, Durham University, UK

Received 12 July 2018; Revised 15 May 2019; Accepted 20 May 2019

*Correspondence to: Robert I. Ferguson, Department of Geography, Durham University, South Road, Durham DH1 3LE, UK. E-mail: r.i.ferguson@durham.ac.uk

ESPL
Earth Surface Processes and Landforms

ABSTRACT: Many models of incision by bedrock rivers predict water depth and shear stress from discharge; conversely, palaeoflood discharge is sometimes reconstructed from flow depth markers in rock gorges. In both cases, assumptions are made about flow resistance. The depth–discharge relation in a bedrock river must depend on at least two roughness length scales (exposed rock and sediment cover) and possibly a third (sidewalls). A conceptually attractive way to model the depth–discharge relation in such situations is to partition the total shear stress and friction factor, but it is not obvious how to quantify the friction factor for rough walls in a way that can be used in incision process models. We show that a single flow resistance calculation using a spatially averaged roughness length scale closely approximates the partitioning of stress between sediment and rock, and between bed and walls, in idealized scenarios. Both approaches give closer fits to the measured depth–discharge relations in two small bedrock reaches than can be achieved using a fixed value of Manning's *n* or the Chézy friction factor. Sidewalls that are substantially rougher or smoother than the bed have a significant effect on the partitioning of shear stress between bed and sidewalls. More research is needed on how best to estimate roughness length scales from observable or measurable channel characteristics. © 2019 John Wiley & Sons, Ltd.

KEYWORDS: bedrock rivers; roughness; shear stress; stress partitioning; sidewalls; hydraulic geometry; friction factor; incision process models; palaeohydrology

## Introduction

An increase in water discharge ($Q$) within a river channel is matched by an increase in the product of water width ($w$), mean flow depth ($d$) and mean velocity ($v$). The relative changes in width and depth depend on the shape of the channel cross-section, and the relative changes in depth and velocity depend on the flow resistance behaviour of the river (Ferguson, 1986; Dingman, 2007). Different assumptions about flow resistance therefore lead to different predicted rates of change of $w$, $d$ and $v$ with $Q$, and different quantitative predictions of flood risk, in-stream habitat and geomorphic processes. In bedrock rivers, which are the particular concern of this paper, assumptions about flow resistance are central to calculations of depth and shear stress at a given discharge in landscape evolution models (LEMs) of the stream-power type (e.g. Howard, 1994; Whipple and Tucker, 1999) and in more detailed reach-scale models of incision processes and sediment cover (e.g. Sklar and Dietrich, 2004; Turowski *et al.*, 2007; Lague, 2010; Inoue *et al.*, 2014; Zhang *et al.*, 2015). They are also essential for estimating palaeoflood discharge from the height at which slackwater deposits are preserved on the walls of bedrock gorges (e.g. Baker, 1987; Miller and Cluer, 1998).

Almost all research on these aspects of bedrock river behaviour assumes either the Manning equation

$$v = \frac{R^{2/3} S^{1/2}}{n} \tag{1}$$

or a dimensionally consistent version of the Chézy equation:

$$v = C_f (gRS)^{1/2} = \left(\frac{8gRS}{f}\right)^{1/2} \tag{2}$$

Here and later, $R$ is the hydraulic radius of the river (often approximated by the mean depth $d$), $S$ is the channel gradient, $g$ is the gravity acceleration, $n$ is Manning's roughness coefficient, $C_f = (8/f)^{1/2}$ is the non-dimensional Chézy coefficient and $f$ is the Darcy–Weisbach friction factor. LEMs use a shear stress formulation that implies a spatially and temporally constant value of either $n$ or $C_f$ (e.g. Howard, 1994; Lague *et al.*, 2005). Some process models that include sediment cover and sediment transport rate have used the Manning equation with a Strickler-type relation between $n$ and the 1/6 power of a representative sediment grain size $D$ (e.g. Inoue *et al.*, 2014), while others have assumed a fixed value of $C_f$ (e.g. Chatanantavet and Parker, 2009). A few process models have departed from the standard assumptions and used a logarithmic resistance equation containing a bed roughness height (e.g. Lamb *et al.*, 2008; Nelson and Seminara, 2012). In palaeohydrology, the Manning equation is used at a series of cross-sections to predict the water surface profile, and discharge is varied to obtain the best match to the palaeostage indicators. The value of $n$ is usually the same for each section and invariant with discharge.

The fixed-$n$ and fixed-$C_f$ assumptions are convenient in incision models because they simplify the calculation of depth from discharge. However, both assumptions are questionable. One concern is the use of fixed $n$ or fixed $C_f$ in LEMs and other incision models that allow discharge to fluctuate. The available evidence from flow measurements in bedrock rivers suggests that neither $n$ nor $C_f$ remains constant as discharge increases from low flow to flood conditions; instead, both $n$ and $C_f$ decrease, the latter more strongly (Heritage *et al.*, 2004; Kidson *et al.*, 2006; Richardson and Carling, 2006; Ferguson *et al.*, 2017a). This is also the case (e.g. Reid and Hickin, 2008; Ferguson, 2010) in alluvial channels with coarse beds, which are recognized as having much in common with bedrock rivers (Whipple *et al.*, 2013).

The second problem with assuming a fixed value of $n$ or $C_f$ is the lack of any basis for specifying $C_f$ in terms of observed or assumed characteristics of a bedrock river, and the weakness of specifying $n$ from a grain size when the sediment-free parts of the channel may be far rougher or smoother and the extent of sediment cover may vary over time. This conceptual objection was recognized by Nelson and Seminara (2012), Johnson (2014) and Inoue *et al.* (2014), who proposed using an area-weighted average of separate rock and sediment roughness length scales to estimate depth and bed shear stress in bedrock rivers.

Our aim in this paper is to develop better ways of modelling the bulk hydraulics of bedrock rivers in which there are differences in roughness between rock bed, sediment cover and possibly also sidewalls (Ferguson *et al.*, 2017a). The improvements we seek are a stronger conceptual or physical basis, the ability to specify model parameters from observable channel characteristics and superior predictive performance compared to the fixed-$n$ and fixed-$C_f$ assumptions. We begin by generalizing the weighted-average approach to allow for distinctively rough or smooth sidewalls. We then propose an alternative conceptual approach based on partitioning of the total shear stress (and thus also the total friction factor) and develop a practical calculation method using this approach. We show that these new models give very similar predictions of the depth–discharge relation in simplified representations of two large bedrock rivers, and can closely reproduce the measured depth–discharge relations in two small bedrock reaches for which we have detailed flow measurements. When applied to large-river scenarios, the new models show that distinctively rough or smooth sidewalls can significantly alter the distribution of shear stress between bed and sidewalls. We discuss the implications of our results for incision process models and palaeohydrology, and call for more research on how best to estimate roughness parameters from observable channel characteristics.

## Alternative Conceptual Frameworks

The approach proposed by Nelson and Seminara (2012) is a single flow resistance calculation for the entire cross-section using a composite roughness length scale (denoted hereafter by $k_{av}$) calculated as the area-weighted average of separate $k$ values for exposed rock in the bed ($k_r$) and a partial sediment cover ($k_s$). Thus, if sediment covers a proportion $c$ of the bed, $k_{av} = ck_s + (1 - c)k_r$. Inoue *et al.* (2014) took a similar approach in their model, Johnson (2014) proposed a variant of it and Ferguson *et al.* (2017a) tried it in a discussion of field measurements.

As Johnson (2014) noted, this approach can in principle be generalized to use a weighted average of more than two roughness length scales using the relevant proportions of the wetted perimeter. In a trapezoidal channel with a proportion $c$ of sediment cover on its bed, and sloping sidewalls with a distinctive roughness length scale $k_w$, the area-weighted average roughness is

$$k_{av} = \frac{cw_0k_s + (1 - c)w_0k_r + 2sk_w}{w_0 + 2s} \quad (3)$$

where $w_0$ is the bed width and $s$ is the slant distance up the submerged part of each side wall (so $s = d$ for a rectangular channel). This approach is easily applied to calculations of velocity and discharge at a known depth, but requires iteration if the requirement is to calculate depth from discharge since the value of $s$ is not then known in advance. It can also be criticized as lacking physical basis, even though it is phenomenologically correct in that the overall flow resistance varies according to the extent of different roughness zones.

An alternative conceptual framework with a stronger physical basis is stress partitioning. This approach has long been taken in other fluvial contexts involving two or more distinct sources of resistance. Sand-bed rivers may have dune bedforms as well as grain roughness, torrents often contain rarely mobile boulders and/or large woody debris as well as gravel, and in flume experiments on sediment transport the glass sidewalls are smoother than the bed. In each case the standard conceptual approach is stress partitioning (e.g. Einstein and Barbarossa, 1952; Vanoni and Brooks, 1957; Manga and Kirchner, 2000; Yager *et al.*, 2007), so this is an obvious framework for handling multiple scales of roughness in bedrock rivers.

Both approaches involve area-weighted averaging, but of different variables as shown in cartoon form in Figure 1. In the stress-partitioning approach, three separate calculations are performed to estimate a different friction factor for each $k$ value, and the reach-average friction factor $f$ is then obtained as an area-weighted average of the three individual $f$ values. In the $k_{av}$ approach, the overall $f$ is obtained by a single resistance calculation using the area-weighted average of the different $k$ values. Either way, once $f$ is known it is used in Equation (2) to calculate velocity and discharge if depth and slope are known (as in palaeoflood estimation), or to calculate depth and velocity if discharge and slope are known (as in incision models).

Our suggested stress-partitioning framework for bedrock rivers with three roughness length scales is an extension of the standard Vanoni and Brooks (1957) method for applying a sidewall correction to the bed shear stress in flume experiments with smooth glass walls and a relatively rough sediment bed. The basis of that method is to partition the total boundary shear force per unit channel length as

$$(w + 2d)\tau = w\tau_b + 2d\tau_w \quad (4)$$

where $w$, $d$ are the flume width and flow depth, $\tau$ denotes the total shear stress ($= \rho gRS$) and $\tau_b$, $\tau_w$ are the stresses on the bed and walls, respectively. Since the flume walls are smooth, $\tau_w$ is less than $\tau$ and $\tau_b$ must be higher than $\tau$. In uniform flow the overall mean velocity is $v = (8gRS/f)^{1/2}$, so $\tau = \rho v^2 f/8$. If this last relationship is assumed to apply also to $\tau_b$ and $\tau_w$, it follows that the overall friction factor is given by a weighted average of the bed and wall friction factors, $f_b$ and $f_w$:

© 2019 John Wiley & Sons, Ltd. 

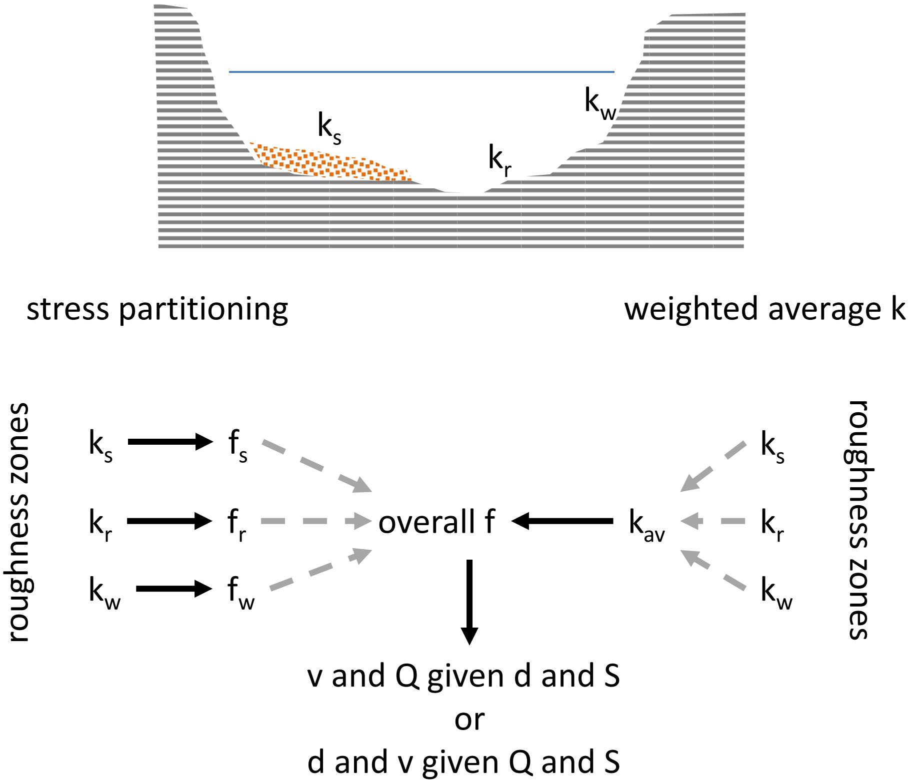


**Figure 1.** Alternative frameworks for calculating the bulk hydraulics of a bedrock reach with different roughness length scales for rock floor ($k_r$), sediment cover ($k_s$) and sidewalls ($k_w$) and either one or three values of the friction factor *f*. Dashed grey arrows denote averaging of the three components, weighted by their areal extent. Black arrows denote assumed physical relations. [Colour figure can be viewed at wileyonlinelibrary.com]

$$f = \frac{wf_b + 2df_w}{w + 2d} \tag{5}$$

In a flume experiment the slope, discharge and depth are either known or easily measured and *f* is therefore also known. Equation (5) can then be solved for $f_b$ (and thus the bed shear stress) by using an estimate of the (low) value of $f_w$ for the glass sidewalls. This estimate is obtained from the smooth-pipe Moody diagram using the Reynolds number of the flow.

Applying this approach to bedrock rivers differs in three ways from the flume sidewall correction problem: we are trying to predict the overall *f* rather than $f_b$, the sidewalls are hydraulically rough not smooth and we need to allow for a partial sediment cover on the rock bed. If the bed friction factor is decomposed into sediment and rock components, $f_s$ and $f_r$, respectively, the overall friction factor in a trapezoidal bedrock channel can be expressed as

$$f = \frac{cw_0f_s + (1-c)w_0f_r + 2sf_w}{w_0 + 2s} \tag{6}$$

where *c*, $w_0$ and *s* again denote cover fraction, bed width and sidewall slant depth. This has the same form as Equation (3): an area-weighted average, but now of friction factors not roughness length scales. The bed friction factors $f_s$ and $f_r$ can be modelled using appropriate roughness length scales in any preferred flow resistance relation, but specifying the sidewall friction factor $f_w$ is more problematic. The value of $f_w$ must depend on the drag coefficient for the particular wall topography and the near-wall velocity $v_w$, but a rigorous fluid-mechanics analysis of flow near undulating walls (Kean and Smith, 2006) concluded that even if the drag coefficient $C_D$ is known, $v_w$ depends also on the overall mean velocity *v*, which is one of the variables we are trying to predict. Similarly, Cheng (2011) derived an equation to predict $f_w$ in flumes with rough vertical walls characterized by a roughness length scale $k_w$, but it requires that the overall friction factor is known whereas we are trying to predict it. An iterative calculation would be possible where depth is known (as in palaeoflood estimation), but it would be impractical as part of a general incision process model. Cheng's equation implies that $f_w$ decreases with increasing hydraulic radius and overall mean velocity, but increases with $k_w$ at any given velocity. This qualitative behaviour can be obtained by calculating $f_w$ from $R/k_w$, which we use as an approximation later, but this has no physical basis and its accuracy is unknown.

## Resistance Equations and Roughness Length Scales

Whether the overall conceptual framework is weighted-average roughness or friction partitioning, the link between the hydraulic variables of interest and the roughness length scales $k_r$, $k_s$ and $k_{av}$ has to be a flow resistance equation in which $C_f$ varies with the relative submergence *R*/*k*. The Manning equation when combined with the Strickler relation $n \propto D^{1/6}$ is of this type, since it can be expressed as $C_f \propto (R/k)^{1/6}$. Johnson (2014) and Inoue *et al.* (2014) both used this resistance model to explore how roughness differences affect the development of sediment cover in bedrock rivers. However, analyses of extensive data compilations of flow measurements in alluvial channels with coarse beds have shown that the Manning–Strickler equation systematically underestimates resistance in shallow flows (Ferguson, 2007; Rickenmann and Recking, 2011). Underestimation of resistance implies overestimation of velocity, and underestimation of depth and total shear stress, at a given discharge. A 'shallow' flow in this context means a depth that is less than about $5D_{84}$, where $D_{84}$ (the 84th

© 2019 John Wiley & Sons, Ltd. 

percentile grain diameter) is the conventional operational definition of $k$ in alluvial channels. Many bedrock rivers are shallow in this sense because of exposed rock ribs and/or large clasts that have fallen in from the sides or been detached from the bed, and as already noted the few published measurements of flow resistance in bedrock rivers all show that $n$ decreases with increasing discharge at a site.

Ferguson (2007) and Rickenmann and Recking (2011) analysed large compilations of flow data from gravel- and boulder-bed channels and found that the best fit to the trend of the relation between $C_f$ and $R/D_{84}$ is obtained using either of two relative submergence resistance equations that are not simple power laws. The first is the logarithmic relation

$$C_f = \left(\frac{8}{f}\right)^{1/2} = \frac{1}{\kappa}\ln\left(\frac{aR}{k}\right) \quad (7)$$

where $\kappa \approx 0.4$ is von Karman's constant and $\alpha \approx 12 \pm 1$ depending on channel cross-section shape (Keulegan, 1938; Hey, 1979). This relation is derived by integrating the logarithmic 'law of the wall' for velocity profiles in turbulent boundary layers. The roughness height $k$ is equated with grain size for uniform sediment but has to be increased to a multiple of $D_{84}$ or $D_{90}$ for the best fit to data from gravel-bed rivers (e.g. Bray, 1979; Hey, 1979; Ferguson, 2007). As noted above, Lamb *et al.* (2008) and Nelson and Seminara (2012) used this type of relation in process models of bedrock rivers.

The other alternative is the variable power equation (VPE) proposed by Ferguson (2007):

$$C_f = \frac{a_1 a_2 (R/k)}{\sqrt{a_1^2 + a_2^2 (R/k)^{5/3}}} \quad (8)$$

This is a smooth link between two asymptotes: for deep flows the Manning–Strickler relation $C_f = a_1(R/k)^{1/6}$ and for very shallow flows the roughness layer relation $C_f = a_2 R/k$ that was implied by results in Rickenmann (1991) and Aberle and Smart (2003). The coefficients take best-fit values $a_1 \approx 6.5$ and $a_2 \approx 2.5$ when $k$ is equated with $D_{84}$. Equations (7) and (8) give very similar results in most rivers, but the VPE works marginally better in extremely shallow flows (Ferguson, 2007; Rickenmann and Recking, 2011). It has been adopted in several studies of steep torrents (e.g. Nitsche *et al.*, 2012; Schneider *et al.*, 2015), and Lamb *et al.* (2017) found it closely matched flow over a rough planar bed in a steep flume. The VPE with coefficients 6.5 and 2.5 was used for all calculations reported later in the paper, but with different relative submergence ratios depending on the context: $R/k_s$ for a separate calculation of flow over a partial sediment cover, $R/k_r$ for a separate calculation of flow over exposed rock in the bed, $R/k_w$ for a separate calculation for the sidewalls or $R/k_{av}$ for a single calculation using an area-weighted average of two or three different roughness length scales. We repeated some of the calculations using Hey's (1979) logarithmic relation, which uses $k = 3.5D_{84}$, as a sensitivity check and obtained similar results when our $k$ values were inflated by a factor of 3.5.

The final choice when applying any model that uses roughness length scales is how to estimate the $k$ values. As already noted, the length scale for bed sediment, $k_s$, is generally based on a grain diameter from the coarse tail of the size distribution. The alternative is to use the topographic standard deviation of bed elevation ($\sigma_z$ hereafter) as derived from a digital elevation model after removing the overall channel gradient and any other large-scale trend. This is conceptually attractive since the same grain size distribution can give a rougher or smoother surface depending on how the grains are packed. Aberle and Smart (2003) found that using $\sigma_z$ instead of $D_{84}$ gave a better log-law fit to the measured flow in flume experiments with coarse beds and slopes of 2–10%. The topographic standard deviation is also the only obvious way to characterize the roughness of exposed bedrock. It has been used for this in flume experiments with concrete 'bedrock' (e.g. Finnegan *et al.*, 2007), in bedrock process models (e.g. Johnson, 2014) and in analyses of sediment transport (Hodge *et al.*, 2011) and flow resistance (Ferguson *et al.*, 2017a) in natural channels. We are not aware of any published work on estimating the roughness length scale $k_w$ for rock sidewalls, but conceptually it should again be related to the topographic irregularity of the walls.

## Comparison of Models: Idealized Scenarios

The literature review and theory earlier in the paper can be summarized as follows: stress partitioning is conceptually attractive but there is no convenient physically based way to apply it to channels with rough sidewalls, whereas the weighted-average roughness approach lacks physical basis but is easy to apply. But how much practical difference is there between the two approaches in situations where both can be applied with confidence? To answer this question, we made calculations for simplified representations of two large bedrock channels that have been described in the literature: the Liwu River in Taiwan and the Fraser Canyon in western Canada. The same scenarios are used later to investigate how sidewall roughness affects the bed and sidewall shear stresses.

The Liwu River has been the scene of much research on incision rates and fluctuations in sediment supply and evacuation (e.g. Hartshorn *et al.*, 2002; Turowski *et al.*, 2008), and Lague (2010) used a simplified representation of its channel in his generic simulation of long-term cover variation and incision rate. We adopt his geometry here. The river is represented as a trapezoidal channel with bed width 30 m, 60° sidewalls and a 2% gradient. We made calculations for discharges of 100 and 1000 $m^3\ s^{-1}$, which correspond to moderate flood conditions and slightly above the mean annual flood.

The middle course of Fraser River runs through a series of rock-walled canyons along a fault zone between the Coast Mountains and Cascade Mountains. The morphology of reaches with two, one or no rock walls is described and contrasted by Rennie *et al.* (2018). As for the Liwu River, we represent rock-walled reaches of the Fraser River by a trapezoidal channel with 60° sidewalls, but now with a gradient of 0.1% and a bed width of 100 m (based on data in Figure 8 of Rennie *et al.*, 2018). We made calculations for discharges of 3000 and 10 000 $m^3\ s^{-1}$; for comparison, the mean discharge and mean annual flood at the downstream end of the canyons are approximately 2700 and 8700 $m^3\ s^{-1}$.

To determine whether the two methods predict substantially different mean flow depths for a given discharge, we made calculations for both rivers on the assumption of a 50% sediment cover that does not vary with discharge and a factor of 4 difference between the roughness length scales for exposed rock and sediment cover (e.g. $k_{av}$ = 1 m was achieved by setting one roughness length to 0.4 m and the other to 1.6 m). This ratio was used because it is well within the range of what can be found in bedrock rivers, particularly those with smooth rock beds, but should be sufficient to reveal any strong sensitivity of predicted depth to calculation method. In the absence of published information on the roughness of the beds of either river, we repeated the calculations for several different values of $k_{av}$. This also allowed comparison of differences in depth

© 2019 John Wiley & Sons, Ltd. 

according to flow resistance model with differences in depth according to overall bed roughness. The depth for each given discharge was obtained first by a single VPE calculation using $R/k_{av}$ and then by the stress partitioning approach with $f_s$ and $f_r$ computed separately using the VPE with $R/k_s$ and $R/k_r$, respectively. In each case the calculation started with a trial value of the depth and ended with a discharge value; the depth was then adjusted to obtain the target value of the discharge.

The results show that depth depends far more on discharge and overall roughness than on the calculation method (Figure 2). The percentage difference between the depths calculated using the $k_{av}$ and stress-partitioning methods increases with the average roughness of the bed, but over the range of conditions we considered it is always small: 2–6% at the lower discharge in each river, and 1–4% at the higher discharge. These differences in depth according to calculation method would be even smaller if the contrast in roughness was lower, eventually disappearing in the limit of no difference in roughness. Even with the factor of 4 ratio of roughness lengths used here, the differences in depth according to calculation method are far smaller than the changes in depth when the average bed roughness is altered (Figure 2). This numerical experiment provides a clear answer to the question posed at the start of this section: the depth–discharge relation in the scenarios considered is much less sensitive to the choice of calculation method than to the overall roughness of the channel.

## Comparison of Models with Field Measurements

As a test of our new models, we investigated how well they could reproduce the measured depth–discharge relations in two contrasting reaches of Trout Beck, a small stream in the Pennine hills of northern England. The channel, its geological setting and hydrology, and the field measurements made are described at length in Ferguson *et al.* (2017a, 2017b). The site is a 0.3 km long gorge where Trout Beck, which has a local

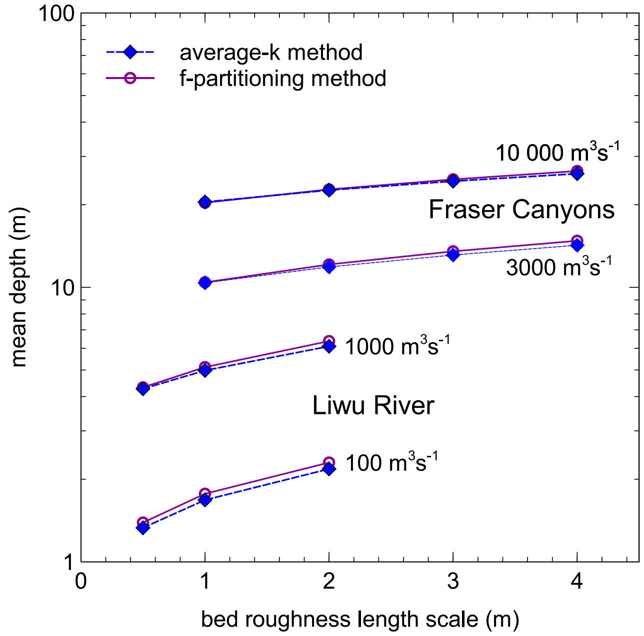


**Figure 2.** Predicted depths in idealized representations of two bedrock rivers with a factor of 4 difference in roughness between two halves of the bed. Depth is shown as a function of discharge, mean roughness and calculation method. [Colour figure can be viewed at wileyonlinelibrary.com]

channel gradient of about 2%, cuts through a thin band of massive limestone in an otherwise less resistant sedimentary sequence dipping at less than 2%. We measured cross-sections and water levels in four short reaches of the gorge and one alluvial reach immediately upstream, and used the discharge record from a nearby gauging station to calculate reach-average velocity and flow resistance over a range of discharge from <0.1 to 9 m$^3$ s$^{-1}$; for comparison, the mean discharge is ~0.4 m$^3$ s$^{-1}$ and the mean annual flood is ~11 m$^3$ s$^{-1}$. Details of the methods are in Ferguson *et al.* (2017a). Here we consider two reaches, one (reach F2) with negligible sediment cover and the other (reach F3) a short way downstream with 70% cover. The sediment cover was mapped during low-flow conditions before, during and after the period of flow measurement. No overall change was detected. It is possible that transient changes in cover occur during major flood events, but we do not think this occurred to any significant extent in the study period, which did not include any major floods. A tracer-pebble experiment reported in Ferguson *et al.* (2017b) showed that sediment is flushed through reach F2 even in moderate (~2 m$^3$ s$^{-1}$) discharges and that tracers entering reach F3 had lower mobility than anywhere else in the 0.3 km-long gorge. We accordingly treated the 0 and 70% cover fractions as invariant in the main calculations reported below, though we do discuss to what extent within-event changes might affect the results.

### Reach characteristics

The morphology of the two reaches is illustrated in Figure 3. Each reach is about 25 m long, they are 30 m apart and have bankfull widths of about 6 m (F2) and 7 m (F3). Because the stream is flowing almost along the dip, the rock bed of reach F2 is notably smooth apart from small steps and a shallow inner channel. We do not have detailed measurements of rock roughness in F2, but Hodge and Hoey (2016) made a laser scan of an 18 × 9 m area about 200 m downstream and still on the same limestone bed. Analysis of the digital elevation model obtained from that scan showed that the standard deviation ($\sigma_z$) of detrended rock bed elevation increases from 0.06 to 0.10 m as the averaging area used increases from 3 × 3 m to 9 × 9 m (Ferguson *et al.*, 2017a).

Both reaches have rock sidewalls with a much more irregular topography than the bed of F2. The walls are stepped in cross-section with an alternation of rounded ledges and near-vertical parts (Figure 3, top left). In plan view, the near-vertical parts have angular protrusions and embayments with an amplitude of up to nearly 1 m where large blocks have been removed. Flow separates at the protrusions and recirculates within the embayments (Figure 3, lower image). Since topographic irregularity in the streamwise direction is the main source of flow resistance, we infer that the sidewall roughness length scale ($k_w$) in F2 and F3 is a few to several decimetres (i.e. considerably greater than the bed roughness length scale). The sediment cover in reach F3 is coarse. A 100-clast Wolman-type pebble count gave an estimated median diameter ($D_{50}$) of 84 mm and a $D_{84}$ of 191 mm. As can be seen (Figure 3, top right) the reach contains a large number of boulders, with diameters up to 1.1 m and a mean spacing of ~1 m.

The measured changes in mean flow depth and flow resistance as discharge increases in the two reaches were reported in Ferguson *et al.* (2017a) and are reproduced here for convenience (Figure 4). In both reaches there is a kink in the depth curve at a discharge just below 2 m$^3$ s$^{-1}$. Above this level, water rises up the irregular sidewalls and depth increases more rapidly than at lower discharges, especially in F2. Velocity

© 2019 John Wiley & Sons, Ltd. 

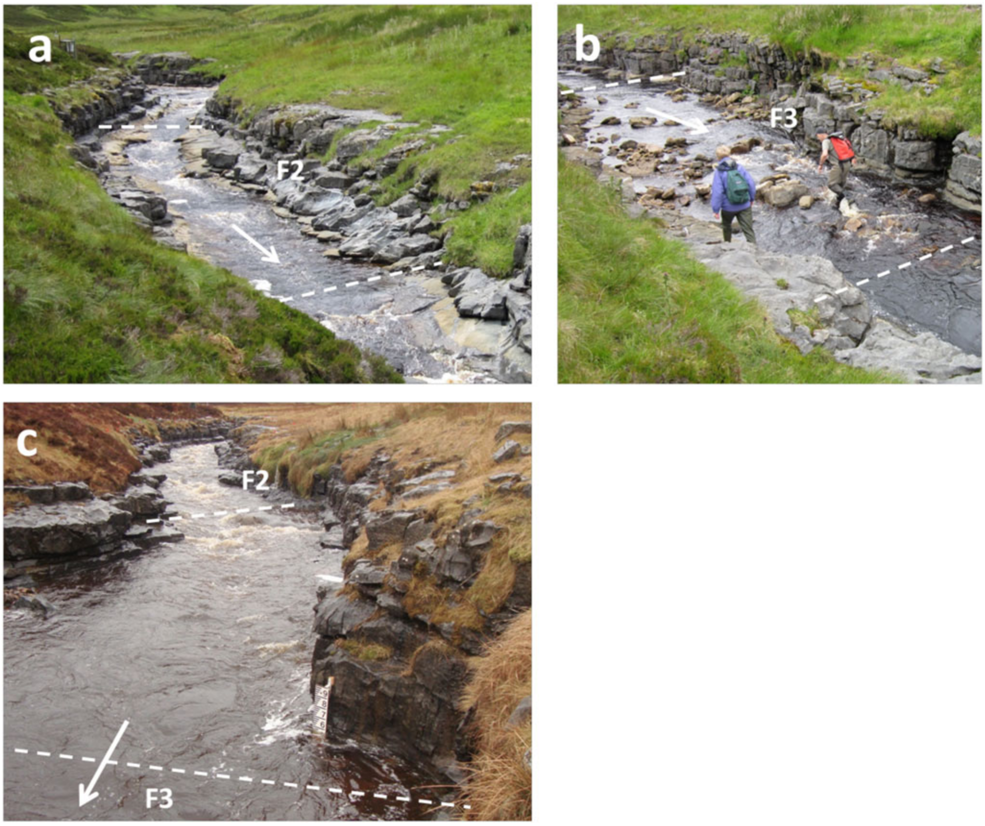


**Figure 3.** Views of reaches F2 and F3 of Trout Beck at low flow (upper) and ~2 $m^3 s^{-1}$ (lower) to illustrate their morphology, sediment cover, and bed and sidewall rock roughness. Bankfull widths are 6 to 7 m. Field measurements of hydraulic variables were averaged over the distance between the dashed lines in the upper images. [Colour figure can be viewed at wileyonlinelibrary.com]

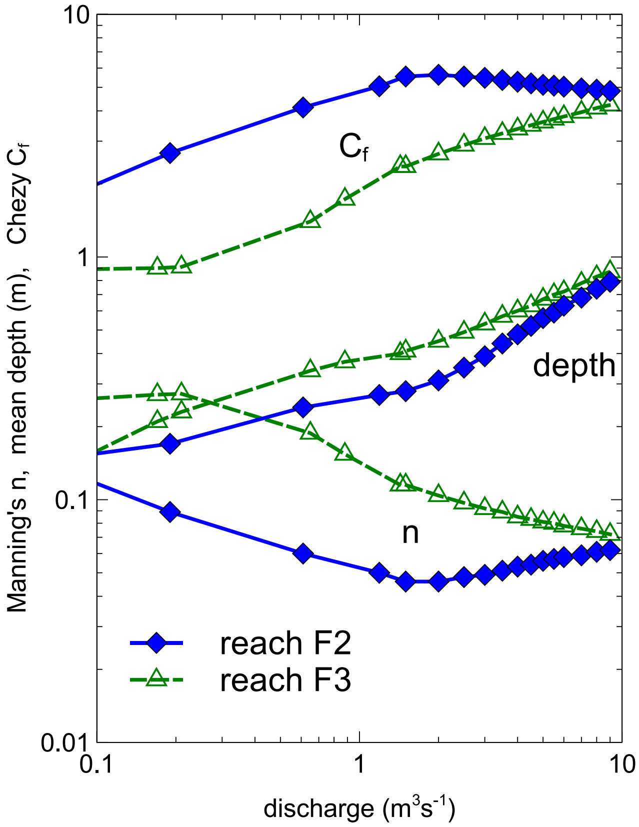


**Figure 4.** Measured changes in reach-average mean depth and flow resistance as discharge increases in two reaches (F2 and F3) of Trout Beck. [Colour figure can be viewed at wileyonlinelibrary.com]

(not shown) does the opposite, increasing more slowly at high discharges. Flow resistance as quantified by $n$ is very high in F3 at low discharges, but decreases progressively as the stream rises. Resistance in F2 is considerably lower than in F3 at most discharges, as expected for a smooth rock bed without the coarse sediment that covers most of F3, but at discharges above 2 $m^3 s^{-1}$, $n$ increases as the stream rises up the rough sidewalls. The reach-averaged friction factor $f$ (not shown) varies in the same way as $n$ in both reaches, but over a greater range. $C_f$ consequently increases monotonically in F3 but undergoes a reversal in F2, increasing at low flow but decreasing in flood conditions.

## Application of alternative flow resistance models

We have data on mean flow depth, energy slope and other bulk hydraulic variables in both reaches at 17 distinct water discharges from <0.1 to 9 $m^3 s^{-1}$. To determine how well alternative flow resistance models can reproduce the measured depth–discharge relation in each reach, we used them to predict the mean velocity and thus estimate the discharge $Q = wdv$ for comparison with the known value. The traditional fixed-$n$ and fixed-$C_f$ resistance models allow direct calculation of velocity from hydraulic radius and slope. For the $k_{av}$ model, the overall friction factor at each depth was calculated using the VPE [Equation (8)] with $R/k_{av}$, and $v$ and $Q$ could then be calculated. The level at which the sidewalls begin was determined by sharp kinks in plots of measured mean depth against flow width and corresponds to a discharge of 2 $m^3 s^{-1}$ in F2 and 1.5 $m^3 s^{-1}$ in F3. In the stress-partitioning model, the rock bed, sediment cover and sidewall friction factors were

© 2019 John Wiley & Sons, Ltd. 

estimated using the VPE, with $R$ divided by the relevant roughness length scale, then combined to give the overall friction factor and hence $v$ and $Q$. Each model thus generated a unique depth–discharge relation, and the various relations could be compared with each other and with the measured hydraulic geometry shown in Figure 4.

Since the aim is to see how well the depth–discharge relation can be modelled using observable channel characteristics, our initial calculations were done using roughness length scales based on the field observations mentioned in the site description. We set $k_r$ to the midpoint (0.08 m) of the scale-dependent $\sigma_z$ value from farther downstream, and a Strickler-type calculation using this value of $\sigma_z$ gave a trial value of $n = 0.032$ for the sediment-free reach F2. The 'few to several decimetre' sidewall roughness ($k_w$) in the $k_{av}$ and $f$-partitioning models was set to 0.3 m as a rough estimate for initial calculations. For the sediment cover in reach F3, we equated $k_s$ with the $D_{84}$ value of 0.191 m, since the VPE was calibrated for use with $R/D_{84}$ in alluvial rivers, and set $n$ to 0.037 based on a Strickler-type calculation from this $D_{84}$. Some of the calculations were repeated with one or more of the model parameters adjusted to minimize an error metric that is defined below. The fixed-$C_f$ models of both reaches were optimized from the start, since there is no way to specify $f$ directly from measured roughness.

The metric used to quantify goodness of fit when comparing or optimizing models was the root mean square (rms) of errors defined as

$$e_i = \log_{10}Q_{mi} - \log_{10}Q_{pi} \quad (9)$$

where $Q_{mi}$ denotes the measured discharge at the $i$th depth and $Q_{pi}$ the predicted discharge at that depth. The use of logarithms avoids the fit being biased almost entirely to the highest discharges. The errors so defined can be visualized as horizontal residuals in the standard log–log plot of $d$ against $Q$. This is the logical way to represent error in models for palaeoflood estimation in channels with rough walls. From the perspective of modelling incision processes and sediment cover variation, one would ideally compare the rms error of predicted depths for given discharge values, but it is not then possible to set up explicit calculations and this prevents the simultaneous optimization of two or more roughness parameters. The relative goodness of fit of alternative models should be the same either way, since we presume that lower rms error in predicting $Q$ from observed $d$ corresponds to lower rms error in predicting $d$ from known $Q$.

## Results

We discuss the sediment-free rock gorge (F2) first as being the simpler case, then consider F3 where the sediment cover introduces a third roughness length scale.

The simulated depth–discharge relations for F2 are illustrated in Figure 5, with parameter values and goodness-of-fit metrics in Table I. The fit of the Manning equation to F2 with $n$ based on rock-bed $\sigma_z$ is poor (Figure 5a), with discharge overpredicted by a factor of 2 or more at all depths. This corresponds to under-prediction of depth at known discharge and implies that the actual flow resistance is much higher than that $n$ value suggests. The best fit with an optimized value of $n$ still overestimates discharge in shallow flows, and now underestimates moderate discharges, but at high discharges it gives a close fit to the data. The same is true of the optimized fixed-$C_f$ fit. These good fits at higher discharges are possible because the measured $n$ and $f$ in this reach remain nearly constant

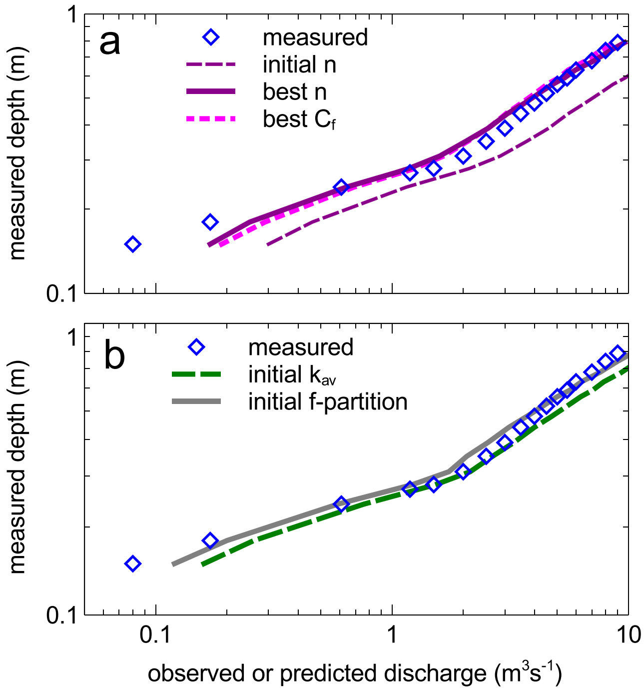


**Figure 5.** Fits of different resistance models to the measured depth–discharge relation in reach F2 of Trout Beck. Symbols show the known discharge at each measured depth; curves show the discharge predicted by each model. See Table I for parameter values and goodness-of-fit metrics. The best fits of the $k_{av}$ and $f$-partitioning models are not shown since they are visually almost identical to the initial fits. [Colour figure can be viewed at wileyonlinelibrary.com]

**Table I.** Goodness of fit of alternative flow models in Trout Beck reach F2

| Method | Rms error in log $Q$ | Parameter values |
|---|---|---|
| Initial fixed $n$ | 0.277 | $n = 0.032$ |
| Best-fit fixed $n$ | 0.104 | $n = 0.058$ |
| Best-fit fixed $C_f$ | 0.123 | $f = 0.31$ ($C_f = 4.7$) |
| Initial $k_{av}$ model | 0.122 | $k_r = 0.08$ m, $k_w = 0.30$ m |
| Best-fit $k_{av}$ model | 0.064 | $k_r = 0.11$ m, $k_w = 0.49$ m |
| Initial $f$-partitioning | 0.067 | $k_r = 0.08$ m, $k_w = 0.30$ m |
| Best-fit $f$-partitioning | 0.067 | $k_r = 0.11$ m, $k_w = 0.36$ m |

(declining slightly then rising slightly) over this range of discharge (Figure 4). However, the best-fit value of $n$ (Table I) is almost double the initial estimate based on rock-bed $\sigma_z$, and could only be predicted in a Strickler-type calculation by assuming an implausibly high $k$ value of well over 2 m.

In contrast, the $f$-partitioning model with our initial estimates of the rock bed and sidewall roughness length scales fits the data very well (Figure 5b), with a much lower rms error than the optimized fixed-$n$ and fixed-$C_f$ models (Table I). The $k_{av}$ model with initial $k$ values gives an excellent fit at intermediate discharges but slightly overestimates low and high discharges, corresponding to underestimation of depth at a given true discharge (Figure 5b). Optimizing the bed and sidewall $k$ values in the $f$-partitioning model makes no visible difference to the already excellent fit and reduces only the fourth significant digit of the rms error (Table I). Optimizing $k_r$ and $k_w$ in the $k_{av}$ model brings the depth–discharge curve indistinguishably close to the $f$-partitioning fit, so for clarity it is not shown in Figure 5. The best fit of both models is obtained with a bed roughness of 0.11 m (Table I), which is only just outside the 0.06–0.10 m range of rock-bed $\sigma_z$ measured 200 m away. The optimized

© 2019 John Wiley & Sons, Ltd. 

$k_w$ values (0.36 and 0.49 m) are higher than our very approximate visual estimate of 0.3 m but not inconsistent with it, and as expected they are much higher than $k_r$.

The depth–discharge relations predicted for reach F3 are shown in Figure 6, with parameter values and goodness-of-fit metrics in Table II. The fit of the Manning equation with $n$ estimated from the measured $D_{84}$ of the sediment cover is very poor (Figure 6a), with low discharges overestimated by a factor of >5 and high discharges by a factor of >2. The fit remains poor even when $n$ is optimized, and the same is true of the fit using an optimized fixed value of $C_f$. These traditional models underestimate flow resistance at low discharges and overestimate it at high discharges, giving the wrong slope for the depth–discharge relation (Figure 6a). This inability to fit the data using a constant value of $n$ or $C_f$ is inevitable given the strong observed decline in both $n$ and $f$ as discharge increases in this reach (Figure 4).

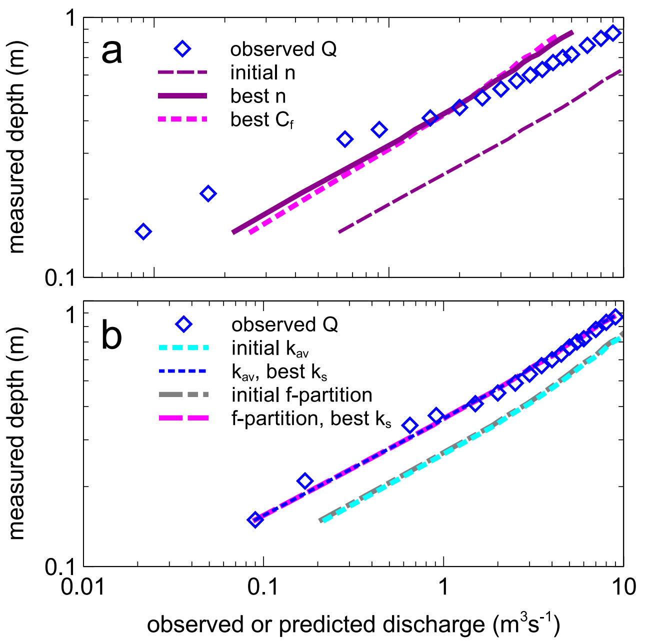


**Figure 6.** Fits of different resistance models to the measured depth–discharge relation in reach F3 of Trout Beck. Symbols show the known discharge at each measured depth; curves show the discharge predicted by each model. See Table II for parameter values and goodness-of-fit metrics. The 'best $k_s$' fits use the initial values of the rock bed and sidewall roughness length scales, but an optimized sediment roughness length scale. The overall best fits of the $k_{av}$ and $f$-partitioning models are not shown since they are visually identical to the best-ks f-partitioning fit. [Colour figure can be viewed at wileyonlinelibrary.com]

**Table II.** Goodness of fit of alternative flow models in Trout Beck reach F3

| Method | Rms error in log $Q$ | Parameter values |
|---|---|---|
| Initial fixed $n$ | 0.493 | $n$ = 0.037 |
| Best-fit fixed $n$ | 0.183 | $n$ = 0.109 |
| Best-fit fixed $C_f$ | 0.214 | $f$ = 1.23 ($C_f$ = 2.6) |
| Initial $k_{av}$ model | 0.291 | $k_s$ = 0.19 m, $k_r$ = 0.08 m, $k_w$ = 0.30 m |
| $k_{av}$ model, best-fit $k_s$ | 0.056 | $k_s$ = 0.54 m, $k_r$ = 0.08 m, $k_w$ = 0.30 m |
| $k_{av}$ model, fully optimized | 0.047 | $k_s$ = 0.57 m, $k_r$ = 0.11 m, $k_w$ = 0.00 m |
| Initial $f$-partitioning | 0.278 | $k_s$ = 0.19 m, $k_r$ = 0.08 m, $k_w$ = 0.30 m |
| $f$-partitioning, best $k_s$ | 0.055 | $k_s$ = 0.48 m, $k_r$ = 0.08 m, $k_w$ = 0.30 m |
| $f$-partitioning, fully optimized | 0.050 | $k_s$ = 0.50 m, $k_r$ = 0.10 m, $k_w$ = 0.00 m |

The depth–discharge fits using the $k_{av}$ and $f$-partitioning approaches are almost identical to each other (Figure 6b, Table II) and have the right slope. However, the fits using our initial values for the three roughness lengths are systematically biased (Figure 6b): the predicted discharge for a given depth is too high, implying that the actual flow resistance is considerably higher than these roughness lengths suggest. Since this reach has 70% sediment cover the dominant roughness scale is $k_s$, and equating $k_s$ with the sediment $D_{84}$ clearly underestimates the resistance of the boulder-rich sediment cover. The fits of the $k_{av}$ and $f$-partitioning models are greatly improved by optimizing $k_s$ alone while retaining the initial field-based estimates of $k_r$ and $k_w$. The simulated depth–discharge curves in Figure 6 b are now very close to the measured relation at all discharges, and the rms errors of these fits (Table II) are comparable to the best fits of the same models to reach F2. In both models the best-fit value of $k_s$ is nearly three times the measured $D_{84}$.

Attempting to optimize all three parameters simultaneously revealed an identifiability problem: the rms error can be reduced slightly by many different combinations of changes in the $k$ values, and the greatest reduction required $k_w \rightarrow 0$ (Table II), which is physically unrealistic. These overall best fits are visually indistinguishable from the 'best $k_s$' fits and are not shown separately in Figure 6b.

We also experimented with variable sediment cover in this reach, and found that a gradual decrease in cover as discharge increases gave a slight improvement in the fit of the $f$-partitioning model with initial values of $k_r$ and $k_w$ but $k_s$ optimized. However, the reduction in rms error is tiny compared to the effect of optimizing $k_s$ (0.003 compared to 0.23), and the tracer-pebble evidence summarized above suggests that if cover in this reach changes at all during events it is more likely to increase than decrease.

## Effect of sidewalls on flow depth and shear stress distribution

Since friction partitioning is equivalent to stress partitioning, any difference in roughness between bed and sidewalls must affect the shear stresses on these two components of the channel perimeter. Our final set of calculations used the $k_{av}$ model to investigate this. We simulated flow in the idealized Liwu and Fraser geometries at the same moderate and major flood discharges as before, but now with a homogeneous bed and relatively rough or smooth sidewalls. We characterized the bed as a whole by an average roughness length scale $k_b$, without distinguishing between exposed rock and sediment cover, and calculated the flow with three alternative values of the sidewall roughness length scale $k_w$: the same as $k_b$ as a control case, and increased or reduced by a factor of 2.

For each roughness scenario we assigned a trial depth, calculated the overall friction factor using $R/k_{av}$ in the VPE, and thus obtained the mean velocity and discharge. The depth was then adjusted to give the target discharge. The total shear stress is $\tau = \rho gRS$, the mean bed shear stress was calculated as $\tau_b = \rho v^2 f_b/8$ with $f_b$ obtained using $R/k_b$ in the VPE and the mean sidewall shear stress was determined by subtracting the bed shear force from the total shear force as in Equation (4). Repeated calculations using the $f$-partitioning approach showed the same qualitative patterns, with very similar (difference ≤

© 2019 John Wiley & Sons, Ltd.

3%) values of depth, total shear stress and bed shear stress but slightly bigger differences in the sidewall shear stress.

The results in Figure 7 are for one particular value of the bed roughness length scale ($k_b$) for each river; calculations using half or twice this value generated similar curves to those shown but shifted up (higher $k_b$) or down (lower $k_b$) by approximately 10%. In the control case the mean bed and sidewall shear stresses are the same as the total shear stress whichever calculation method is used. With $k_w = 2k_b$ (sidewalls rougher than bed), the depth and total shear stress are slightly higher than in the control case, the bed shear stress is considerably lower and the wall shear stress is considerably higher. With $k_w = k_b/2$ (sidewalls smoother than bed), the changes are in the opposite direction and more modest in absolute terms, though comparable in terms of percentage change. Depth and total shear stress are slightly lower than in the control case, the shear stress on the sidewalls is lower than in the control case and that on the bed is correspondingly increased. As would be expected, this is the same qualitative pattern as in a glass-walled flume.

## Discussion

Bedrock rivers normally have a partial sediment cover, and that cover is unlikely to have exactly the same topographic roughness as exposed bedrock. The sidewalls are usually bedrock or colluvium rather than fluvially transported sediment, and their topographic roughness need not be the same as either part of the bed. In our Trout Beck field site a difference between rock bed and rock sidewall roughness exists because the stream flows almost along the dip of the sedimentary rock, but its walls have protrusions and embayments where large joint blocks have been detached. A similar situation could arise in jointed igneous rocks, for example where channels are incised into near-horizontal lava flows as described by Baynes *et al.* (2015). Differences between bed and wall irregularity and roughness are also possible in channels incised into tilted sedimentary or metamorphic rocks. The walls might then be either rougher or smoother than the bed, depending on the dip angle and direction of the bedrock and the extent to which irregularities in the rock bed are smoothed by a partial sediment cover filling depressions.

We have developed two possible frameworks for modelling the depth–discharge relation in a bedrock river with multiple roughness length scales: partitioning of the total mean shear stress and thus of the overall friction factor, or a single flow-resistance calculation using the area-weighted average of the separate roughness length scales (Figure 1). Both approaches allow prediction of depth and shear stress if discharge and slope are known or assumed (as in LEMs and incision process models), or of discharge if depth and slope are known (as in palaeohydrology). Applying either framework requires (1) choosing a specific flow resistance equation, (2) deciding whether a different roughness length scale should be used for the sidewalls and (3) specifying the values of the roughness parameters in the chosen model. We discuss these issues in the remainder of the paper, and consider what implications rough sidewalls might have for bedrock river process models and palaeohydrology.

### Choice of conceptual framework

The stress-partitioning approach is conceptually attractive because of its physical basis, and because other composite-roughness situations are often handled in this way: sand-bed rivers with dunes, glass-walled flumes, torrents with large woody debris, and so on. We have shown that it can, in principle, be extended to bedrock rivers in which exposed rock in the bed, the partial sediment cover and the sidewalls all have different roughness length scales. There is, however, a practical complication: analyses by Kean and Smith (2006) and Cheng (2011) suggest that the sidewall friction factor $f_w$ depends on the overall friction factor (or, equivalently, the mean velocity), so that the velocity for a given depth can only be determined by iteration. Our simulations using this approach therefore used an approximate sub-model for $f_w$ that gives the theoretically correct qualitative behaviour. This gave excellent fits in Trout Beck, even though it lacks physical basis. We think this confirms the potential of the approach, but at present are unsure whether to recommend it for practical applications.

The alternative is to use the simpler average-*k* approach first proposed by Nelson and Seminara (2012), which appears to give a close approximation to the results obtained using friction partitioning. We have two lines of evidence for this. First, our calculations for idealized scenarios based on the Liwu River and Fraser Canyon show that the depths predicted by the two methods differ by no more than a few percent when only two roughness scales are involved, whether bedrock and sediment cover with a factor of 4 difference in *k* (Figure 2) or bed and

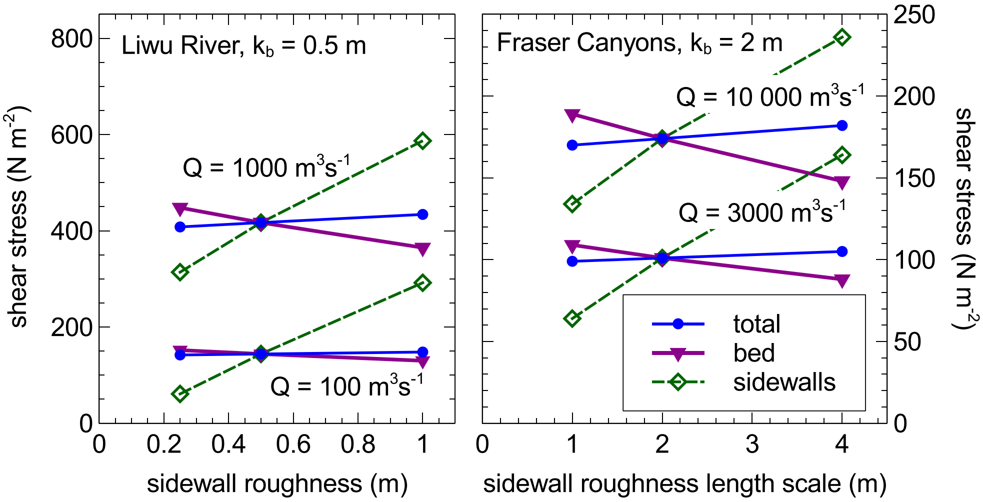


**Figure 7.** Effect of relatively rough or smooth sidewalls on the partitioning of total shear stress in idealized approximations of two large bedrock rivers. [Colour figure can be viewed at wileyonlinelibrary.com]

© 2019 John Wiley & Sons, Ltd. 

sidewalls with a factor of 2 difference (discussion of Figure 7). Second, the fits of the *f*-partitioning and average-*k* models to the measured depth–discharge relations in contrasting reaches of Trout Beck are very similar, whether using our initial estimates of the roughness lengths or optimized values (Figures 5 and 6). And since both fits match the observed relation closely, it can be presumed that a more accurate calculation of the sidewall friction factor would not change the *f*-partitioning fit significantly and it would remain very close to the average-*k* fit and the field data.

We conclude, therefore, that an area-weighted average of two, three or potentially more roughness length scales for different parts of the wetted perimeter is a robust way to allow for differences in frictional resistance to flow. This does, however, require that each distinctive roughness length scale can be associated with a distinct part of the channel perimeter in order to calculate an area-weighted average. It would not, for example, be appropriate to use the average-*k* approach in a sand-bed river with dunes, where both grain and form resistance exist over the entire bed area. A comparable situation might exist in a bedrock river with boulders arrayed over the whole of a relatively smooth rock bed. Stress partitioning is the preferred approach in such situations.

## Choice of resistance law for use with roughness length scales

If the frictional resistance of some or all of the channel perimeter is parameterized by a roughness length scale $k$, the effects on the flow have to be represented by an equation for $C_f$ as a function of the relative submergence $L/k$, where $L$ is some flow-related length scale. In calculations for the entire channel using $k_{av}$, or separate parts of the bed using $k_r$ and $k_s$, $L$ should strictly be the hydraulic radius $R$, though this is often approximated by the mean depth $d$. Our approximate resistance relation for sidewalls also uses $R$. The standard choices for the resistance function are either a logarithmic relation, as used in the first paper to propose using a weighted-average $k$ (Nelson and Seminara, 2012), or the 1/6 power law implied by the Manning equation with $n \propto k_{av}^{1/6}$, as used by Johnson (2014) and Inoue *et al.* (2014).

Our measurements in, and simulations of, Trout Beck suggest that the Manning equation with a fixed *k*-based value of *n* is not always appropriate for bedrock rivers. In reach F3 of Trout Beck, *n* decreases rapidly as the flow depth increases over its 70% cover of coarse sediment. In the sediment-free reach F2, *n* is fairly constant at moderate to high flood discharges, but only because the sidewalls in this reach are rougher than the bed, so that decreasing bed resistance to flow as the water level rises is offset by increased sidewall resistance. This might seem to suggest that the Manning equation is suitable for channels with relatively rough sidewalls, but the *n* value required to give a good match to the data is far higher than can be estimated from the 1/6 power of any plausible roughness length scale for either the bed or the sidewalls.

If a fixed value of *n* is inappropriate, the main alternatives are a logarithmic relation or the VPE [Equations (7) and (8)]. They make almost identical predictions in all but very shallow flows. Both have the inconvenience of not being invertible to allow explicit calculation of depth from discharge in the way that the Manning equation permits. One solution to this problem is to use the non-dimensional hydraulic geometry approximation of the VPE that was devised by Rickenmann and Recking (2011). This allows direct calculation of depth from unit discharge, slope and $D_{84}$, and the latter could be replaced by a $k_{av}$ value. Another possibility is to assume $C_f \propto (R/k)^{1/2}$, which Smart *et al.* (2002) noted as giving a good fit to flume measurements in shallow flows over coarse sediment.

## Significance of sidewall roughness

Relatively rough or smooth sidewalls have a limited effect on the bulk flow in a wide and shallow bedrock river where they make up only a small proportion of the wetted perimeter and may frequently be overtopped. But bedrock rivers are often relatively narrow and deep. Rennie *et al.* (2018) found that reaches of Fraser River with rock walls on both sides were systematically narrower than those with only one, or no, rock sidewall, and the majority of the bedrock channels tabulated by Wohl and David (2008) have a width-to-depth ratio of 6 or less. Sidewalls therefore constitute a substantial part of the wetted perimeter in many bedrock rivers, especially in flood conditions.

Rough sidewalls increase the overall flow resistance so that the river is somewhat deeper and slower than it would be with smoother walls, and has a higher total shear stress. Our calculations for idealized channels modelled on the Liwu River and Fraser Canyon suggest this effect is quite small: increasing the sidewall roughness length scale to twice the average roughness of the bed increases mean depth and total shear stress by only a few percent at a given discharge (Figure 7). But differential roughness has a substantial effect on the partitioning of total shear stress between bed and sidewalls (Figure 7). Increasing the sidewall roughness length scale to twice that of the bed causes bed shear stress to be reduced by 10–20% in the Liwu scenario (depending on discharge and bed roughness) and by 8–15% in the Fraser scenario. Conversely, reducing sidewall roughness by a factor of two causes bed shear stress to increase by 5–13% (Liwu) or 5–9% (Fraser). The mean shear stress on the sidewalls changes in the opposite direction to that on the bed, and by an even greater percentage.

These simulations are for idealized trapezoidal channels in which the sidewalls have the same roughness at all heights. In reality, the bed is unlikely to be completely flat and the sidewall roughness is likely to increase with height as abrasion becomes less frequent and block collapse more likely. This less abrupt change in roughness would give a more continuous variation in shear stress around the perimeter, as predicted in more detailed models of bedrock channel evolution (e.g. Turowski *et al.*, 2008), but there could still be a big contrast between bed and sidewall shear stresses at high discharges.

The reduction in bed shear stress and increase in sidewall shear stress when walls are rougher than the bed has implications for sediment cover and erosion rate. This is not the place to explore the consequences in detail, but their direction seems clear. A lower bed shear stress at a given discharge implies lower sediment transport capacity, and therefore an increase in the ratio of sediment supply to transport capacity if the supply is assumed to be exogenous. This in turn should increase the sediment cover, which is widely assumed to depend on the supply ratio – even though views differ on the precise form of the dependence (e.g. Sklar and Dietrich, 2004; Turowski *et al.*, 2007). The supply of abrasive tools is unchanged but with less of the bed exposed, the overall rate of bed erosion should decrease. However, this will be offset by an increase in erosion of the protruding parts of the rough sidewalls since they now experience a higher shear stress than the bed.

Some of these consequences may be moderated in the long term by feedback: for example, preferential erosion of sidewalls rather than bed eventually widens the channel, so that the rough sidewalls occupy a smaller proportion of the wetted perimeter. Also, if the sediment is coarser than the roughness length scale of exposed rock in the bed ($k_s > k_r$ in our notation),

© 2019 John Wiley & Sons, Ltd. 

the increase in sediment cover will increase the average bed roughness and reduce the difference between bed and sidewall shear stress. A further complication is that if there is a difference in roughness between rock bed and sediment cover, then a change in cover affects the overall flow resistance and total shear stress to at least some extent. Nevertheless, it seems likely that a contrast between the roughness of rock bed and sidewalls would still have implications for long-term channel evolution and incision rates as well as for steady-state channel width.

These speculations are for the case of sidewalls rougher than the bed. In the opposite case of relatively smooth sidewalls, bed shear stress increases at the expense of sidewall shear stress and the above arguments can be reversed: transport capacity should increase, sediment cover decrease and bed erosion rate increase.

A contrast between the roughness of bed and sidewalls also has implications for the practice of palaeoflood estimation from stage indicators on the walls of bedrock gorges. In reach F2 of Trout Beck, with sidewalls much rougher than the bed, Manning's *n* is fairly constant over a range of flood discharges. This might seem to justify the standard assumption of a fixed value of *n* in the hydraulic models used for palaeoflood reconstruction, but it is still necessary to get the *n* value right. There are often no flow measurements at lower discharges with which to calibrate *n*, which instead is assigned on the basis of sediment grain size or generalized recommendations in handbooks. In Trout Beck, the best-fit *n* value for reach F2 is far higher than we estimated from the measured roughness of the rock bed, which is not representative of the rough sidewalls that become increasingly important in flood conditions. In the opposite scenario, with sidewalls smoother than the (presumably rough) bed, flow resistance is likely to decrease strongly as flow depth increases. The assumption that *n* is invariant with discharge is then unsafe, and there is no obvious way to predict what range of values might be appropriate for palaeoflood conditions. Calculations using a logarithmic resistance equation or the VPE would probably be more reliable in this case, especially if the bed roughness height can be calibrated by observations in low-flow conditions.

### Specifying roughness length scales

Topographic irregularity is the only obvious basis for estimating the roughness length scales of rock beds ($k_r$) and sidewalls ($k_w$). The results of our Trout Beck simulations are encouraging insofar as our initial estimates of $k_r$ and $k_w$ gave good ($k_{av}$ model) to excellent (*f*-partitioning model) fits to the sediment-free reach F2 (Figure 5b), with little or no scope for improvement by optimizing the length scales. The initial estimate of $k_r$ was the mid-range value of the scale-dependent topographic standard deviation obtained by analysis of a laser scan made more than 20 channel widths away from F2. Although F2 and the scan location are on the same limestone bed, there are some visual differences between them: for example, F2 has a small inner channel whereas the scan site does not. It is not therefore a matter of great concern that the best-fit value of 0.11 m for the rock bed of F2 in $k_{av}$ and *f*-partitioning calculations using the VPE is just outside the 0.06–0.10 m range of $\sigma_z$ in the scanned area.

These findings are for a relatively smooth rock bed. Very little research has been done on the topographic roughness of more irregular beds, in which tilted sedimentary or metamorphic rocks are exposed and their orientation and dip angle are likely to affect flow resistance. More research is needed on how best to smooth the macro-topography of a reach in order to obtain a representative value of $\sigma_z$, at what spatial scale to do this and how to allow for any preferred orientation of topographic highs and lows.

Even less research has been done on quantifying sidewall roughness and resistance. Our estimate of 'a few to several decimetres' for the sidewall roughness length scale $k_w$ was based on the assumption that $k_w$ ought to be smaller than the amplitude of plan form irregularity in the sidewalls, but not an order of magnitude smaller. Our initial value of 0.3 m was only a ballpark estimate, but gave a good to excellent fit in reach F2 (Figure 5b), and the best-fit values of 0.49 or 0.36 m remain plausible.

Clearly, though, much remains to be learned about the contribution of rough sidewalls to flow resistance. Rough sidewalls affect the spanwise velocity profile, creating separation zones and wakes and depressing the mean near-wall velocity. This is analogous to what happens in flow over a cobble/boulder river bed, but with the important difference that rock sidewalls generally have zero porosity. For this reason, physically based models for flow over rough sediment beds (e.g. Lamb *et al.*, 2017) are unlikely to be applicable to rock sidewalls. The most relevant work that we are aware of is Kean and Smith's (2006) analysis of flow near alluvial river banks which have a repeated sequence of full-height protrusions whose plan form resembles the Gaussian probability distribution function. In this geometric model the protrusions always have rounded tips, but their aspect ratio (amplitude divided by wavelength) depends on the standard deviation of the distribution. Kean and Smith found that the spatially averaged drag coefficient could be predicted from the aspect ratio, but they did not express their results in terms of an effective roughness length and they showed there is no unique relation between the drag coefficient and the sidewall friction factor $f_w$. The alternative to a theoretical approach is to learn more about the details of flow near irregular sidewalls by numerical experiments using computational fluid dynamics, or flume experiments using scale models of natural bedrock reaches.

Our simulations of F3 show that the problem of estimating roughness length scales from observable channel characteristics also applies to coarse sediment cover. The measured $D_{84}$ of the 70% cover in this reach greatly underestimated the actual flow resistance, whether used in our new models or to estimate Manning's *n*, and the best fits using the new models required $k_s$ to be increased to between two and three times $D_{84}$ (Table II). This is most likely a consequence of the high boulder density in this reach. Boulders that protrude above the water surface generate spill resistance and form drag, and studies have shown that total resistance increases with the areal density of obstacles until skimming flow starts to develop (e.g. Bathurst, 1978; Yager *et al.*, 2007; Nitsche *et al.*, 2012). A stress-partitioning approach that treats boulders separately from mobile sediment on the bed may be appropriate in such situations, especially if the aim is to estimate the effective shear stress available for sediment transport (Yager *et al.*, 2007). It would also be useful to investigate the extent to which the $\sigma_z$ of sediment patches can deviate from their $D_{84}$.

## Conclusions

It is recognized that the partial sediment cover in a bedrock river may be hydraulically rougher or smoother than the exposed rock in the bed, and that this can have consequences for sediment cover (e.g. Nelson and Seminara, 2012; Johnson, 2014). There can also be a contrast between the roughness of the sidewalls and that of the bed. We have developed two alternative conceptual frameworks for modelling the bulk flow in a

© 2019 John Wiley & Sons, Ltd.

bedrock river with multiple roughness length scales, tested them in two reaches whose depth–discharge relations are known and used them to investigate the consequences of relatively rough or smooth sidewalls in idealized representations of two large bedrock rivers. We reach the following conclusions.

1. A stress-partitioning approach generalized from the flume sidewall correction method is possible, but how best to estimate the sidewall friction factor is unclear at present.
2. Using an area-weighted average roughness length scale in a single flow resistance calculation gives very similar results to stress partitioning in idealized scenarios and in simulations of measured flow.
3. To the extent that bedrock rivers resemble coarse alluvial channels with relatively shallow flow, a fixed value of Manning's $n$ or the Chézy friction factor $C_f$ is unlikely to be an accurate model for how depth varies with discharge in a reach. A logarithmic or variable power resistance relation is likely to give more accurate results. An alternative that should be explored is a 1/2-power relative submergence relation, which is invertible to allow direct calculation of depth from discharge.
4. The topographic standard deviation of exposed rock in the bed appears to be a good basis for estimating a roughness length scale, but research is needed on the appropriate averaging scale and how best to de-trend the topography.
5. The effective roughness of the coarse sediment cover in one of our reaches was greatly underestimated by the measured $D_{84}$, and it would be useful to investigate the alternative of using a topographic standard deviation.
6. The roughness length scale of rock sidewalls ought to depend on their topographic irregularity in plan form, but very little is known about this. Flume experiments and computational fluid dynamics simulations may be useful complements to field measurements.
7. In simulations of large bedrock rivers, making the sidewalls rougher than the bed causes a slight increase in depth and total shear stress at a given discharge, a significant reduction in bed shear stress and a significant increase in sidewall shear stress. This has implications for sediment transport capacity, sediment cover and long-term incision rate and channel evolution.

*Acknowledgements*—The Trout Beck flow measurements were made possible by the efforts of Bishnu Sharma and Jeff Warburton. We thank Jeff Prancevic, Dieter Rickenmann, an anonymous reviewer, and Associate Editor Jens Turowski for thoughtful comments that prompted us to do additional research and helped us transform and improve the first version of the paper.

## Nomenclature

- $\alpha$ cross-section shape coefficient [–] in logarithmic resistance equation [Equation (7)]
- $\kappa$ von Karman constant [–] in logarithmic resistance equation [Equation (7)], taken to be 0.41
- $\rho$ water density [M L$^{-3}$], taken to be 1000 kg m$^{-3}$
- $\sigma_z$ standard deviation of bed elevation [L] relative to a smoothed version of the topography
- $a_1$, $a_2$ coefficients in variable power resistance equation [Equation (8)] [–], taken to be 6.5 and 2.5
- $c$ proportion of river bed covered by sediment [–]
- $C_f$ non-dimensional Chézy coefficient, defined by inverting Equation (2) [–]
- $d$ mean flow depth [L]
- $D$ representative grain diameter of sediment cover [L]
- $e$ goodness-of-fit metric, defined in Equation (9) [–]
- $f$ friction factor [–], defined in Equation (2); subscripts $b$, $r$, $s$, $w$ refer to the bed as a whole, exposed rock in the bed, partial sediment cover and walls, respectively
- $g$ gravity acceleration [LT$^{-2}$], taken to be 9.81 m s$^{-2}$
- $k$ roughness length scale [L]; subscripts $b$, $r$, $s$, $w$ refer to the bed as a whole, exposed rock in the bed, partial sediment cover and walls, respectively
- $n$ Manning's friction coefficient [T L$^{-1/3}$], defined by inverting Equation (1)
- $P$ wetted perimeter [L]; subscripts $b$ and $w$ refer to bed and walls, respectively
- $Q$ water discharge [LT$^{-3}$]
- $R$ hydraulic radius [L]
- $S$ channel slope [–]
- $v$ mean velocity [LT$^{-1}$]
- $v_w$ near-wall velocity [LT$^{-1}$]
- $w$ water width [L]

## References

Aberle J, Smart GM. 2003. The influence of roughness structure on flow resistance on steep slopes. *Journal of Hydraulic Research* **41**: 259–269.

Baker VR. 1987. Paleoflood hydrology and extraordinary flood events. *Journal of Hydrology* **96**: 79–99.

Bathurst JC. 1978. Flow resistance of large-scale roughness. *Journal of the Hydraulic Division of the American Society of Civil Engineers* **104**: 1587–1603.

Baynes ERC, Attal M, Niedermann S, Kirstein LA, Dugmore AJ, Naylor M. 2015. Erosion during extreme flood events dominates Holocene canyon evolution in northeast Iceland. *Proceedings of the National Academy of Sciences* **112**: 2355–2360.

Bray DI. 1979. Estimating average velocity in gravel-bed rivers. *Journal of the Hydraulic Division of the American Society of Civil Engineers* **105**: 1103–1122.

Chatanantavet P, Parker G. 2009. Physically based modelling of bedrock incision by abrasion, plucking, and macroabrasion. *Journal of Geophysical Research: Earth Surface* **114**: F04018. https://doi.org/10.1029/2008JF001044.

Cheng NS. 2011. Revisited Vanoni–Brooks sidewall correction. *International Journal of Sediment Research* **26**: 524–528.

Dingman SL. 2007. Analytical derivation of at-a-station hydraulic-geometry relations. *Journal of Hydrology* **334**: 17–27.

Einstein HA, Barbarossa NL. 1952. River channel roughness. *Transactions of the American Society of Civil Engineers* **117**: 1121–1146.

Ferguson RI. 1986. Hydraulics and hydraulic geometry. *Progress in Physical Geography* **10**: 1–31.

Ferguson R. 2007. Flow resistance equations for gravel- and boulder-bed streams. *Water Resources Research* **43**: W05427. https://doi.org/10.1029/2006WR005422.

Ferguson R. 2010. Time to abandon the Manning equation? *Earth Surface Processes & Landforms* **35**: 1873–1876.

Ferguson RI, Sharma BP, Hodge RA, Hardy RJ, Warburton J. 2017a. Flow resistance and hydraulic geometry in contrasting reaches of a bedrock channel. *Water Resources Research* **53**: 2278–2293. https://doi.org/10.1002/2016WR020233.

Ferguson RI, Sharma BP, Hodge RA, Hardy RJ, Warburton J. 2017b. Bed load tracer mobility in a mixed bedrock/alluvial channel. *Journal of Geophysical Research: Earth Surface* **122**: 807–822. https://doi.org/10.1002/2016JF003946.

Finnegan NJ, Sklar LS, Fuller TK. 2007. Interplay of sediment supply, river incision, and channel morphology revealed by the transient evolution of an experimental bedrock channel. *Journal of Geophysical Research: Earth Surface* **112**: F03S11. https://doi.org/10.1029/2006JF000569.

Hartshorn K, Hovius N, Dade WB, Slingerland RL. 2002. Climate-driven bedrock incision in an active mountain belt. *Science* **297**(5589): 2036–2038.

© 2019 John Wiley & Sons, Ltd.

Heritage GL, Moon BP, Broadhurst LJ, James CS. 2004. The frictional resistance characteristics of a bedrock-influenced river channel. *Earth Surface Processes & Landforms* **29**: 611–627.

Hey RD. 1979. Flow resistance in gravel-bed rivers. *Journal of the Hydraulic Division of the American Society of Civil Engineers* **105**: 365–379.

Hodge RA, Hoey TB. 2016. A Froude-scaled model of a bedrock-alluvial channel reach: 1. Hydraulics. *Journal of Geophysical Research: Earth Surface* **121**: 1578–1596. https://doi.org/10.1002/2015JF003706.

Hodge RA, Hoey TB, Sklar LS. 2011. Bed load transport in bedrock rivers: the role of sediment cover in grain entrainment, translation, and deposition. *Journal of Geophysical Research*: *Earth Surface* **116**: F04028. https://doi.org/10.1029/2011JF002032.

Howard AD. 1994. A detachment-limited model of drainage basin evolution. *Water Resources Research* **30**: 2261–2285.

Inoue T, Izumi N, Shimizu Y, Parker G. 2014. Interaction among alluvial cover, bed roughness, and incision rate in purely bedrock and alluvial-bedrock channel. *Journal of Geophysical Research: Earth Surface* **119**: F03018. https://doi.org/10.1002/2014JF003133.

Johnson JP. 2014. A surface roughness model for predicting alluvial cover and bedload transport rate in bedrock channels. *Journal of Geophysical Research: Earth Surface* **119**: 2147–2173. https://doi.org/10.1002/2013JF003000.

Kean JW, Smith JD. 2006. Form drag in rivers due to small-scale natural topographic features: 1. Regular sequences. *Journal of Geophysical Research: Earth Surface* **111**: F04009. https://doi.org/10.1029/2006JF000467.

Keulegan GH. 1938. Laws of turbulent flow in open channels. *Journal of Research of the National Bureau of Standards* **21**: 707–741.

Kidson RL, Richards KS, Carling PA. 2006. Hydraulic model calibration for extreme floods in bedrock-confined channels: case study from northern Thailand. *Hydrological Processes* **20**: 329–344.

Lague D. 2010. Reduction of long-term bedrock incision efficiency by short-term alluvial cover intermittency. *Journal of Geophysical Research: Earth Surface* **115**: F0211. https://doi.org/10.1029/2008JF001210.

Lague D, Hovius N, Davy P. 2005. Discharge, discharge variability, and the bedrock channel profile. *Journal of Geophysical Research: Earth Surface* **110**: F04006. https://doi.org/10.1029/2004JF000259.

Lamb MP, Dietrich WE, Sklar LS. 2008. A model for fluvial bedrock incision by impacting suspended and bed load sediment. *Journal of Geophysical Research: Earth Surface* **113**: F03025. https://doi.org/10.1029/2007JF000915.

Lamb MP, Brun F, Fuller BM. 2017. Hydrodynamics of steep streams with planar coarse-grained beds: turbulence, flow resistance, and implications for sediment transport. *Water Resources Research* **53**: 2240–2263. https://doi.org/10.1002/2016WR19579.

Manga M, Kirchner JW. 2000. Stress partitioning in streams by large woody debris. *Water Resources Research* **36**: 2373–2379.

Miller AJ, Cluer BL. 1998. Modeling considerations for simulation of flow in bedrock channels. In *Rivers Over Rock: Fluvial Processes in Bedrock Channels*, Tinkler KJ, Wohl EE (eds) . American Geophysical Union: Washington, D.C; 61–104.Geophysics Monograph 107

Nelson PA, Seminara G. 2012. A theoretical framework for the morphodynamics of bedrock channels. *Geophysical Research Letters* **39**: L06408. https://doi.org/10.1029/2011GL050806.

Nitsche M, Rickenmann D, Kirchner JW, Turowski JM, Badoux A. 2012. Macroroughness and variations in reach-averaged flow resistance in steep mountain streams. *Water Resources Research* **48**: W12518. https://doi.org/10.1029/2012WR012091.

Reid DE, Hickin EJ. 2008. Flow resistance in steep mountain streams. *Earth Surface Processes & Landforms* **33**: 2211–2240. https://doi.org/10.1002/esp.1682.

Rennie CD, Church M, Venditti JV. 2018. Rock control of river geometry: the Fraser Canyons. *Journal of Geophysical Research: Earth Surface* **123**: 1860–1878. https://doi.org/10.1029/2017JF004458.

Richardson K, Carling PA. 2006. The hydraulics of a straight bedrock channel: insights from solute dispersion studies. *Geomorphology* **82**: 98–125.

Rickenmann D. 1991. Hyperconcentrated flow and sediment transport at steep slopes. *Journal of Hydraulic Engineering* **117**: 1419–1439.

Rickenmann D, Recking A. 2011. Evaluation of flow resistance equations using a large field data base. *Water Resources Research* **47**: W07538. https://doi.org/10.1029/2010WR009793.

Schneider JM, Rickenmann D, Turowski JM, Kirchner JW. 2015. Self-adjustment of stream bed roughness and flow velocity in a steep mountain channel. *Water Resources Research* **51**: 7838–7859. https://doi.org/10.1002/2015WR016934.

Sklar LS, Dietrich WE. 2004. A mechanistic model for river incision into bedrock by saltating bed load. *Water Resources Research* **40**: W06301. https://doi.org/10.1029/2003WR002496.

Smart GM, Duncan MJ, Walsh JM. 2002. Relatively rough flow resistance equations. *Journal of Hydraulic Engineering* **128**: 568–578.

Turowski JM, Lague D, Hovius N. 2007. Cover effect in bedrock abrasion: a new derivation and its implications for the modeling of bedrock channel morphology. *Journal of Geophysical Research: Earth Surface* **112**: F04006. https://doi.org/10.1029/2006JF000697.

Turowski JM, Hovius N, Hsieh ML, Lague D, Chen MC. 2008. Distribution of erosion across bedrock channels. *Earth Surface Processes & Landforms* **33**: 353–363. https://doi.org/10.1002/sp.1559.

Vanoni VA, Brooks NH. 1957. *Laboratory studies of the roughness and suspended load of alluvial streams.* Sedimentation Laboratory, California Institute of Technology: Pasadena, CA.

Whipple KX, Tucker GE. 1999. Dynamics of the stream-power river incision model: implications for height limits of mountain ranges, landscape response timescales, and research needs. *Journal of Geophysical Research* **104**(B8): 17661–17674.

Whipple KX, DiBiase RA, Crosby BT. 2013. Bedrock rivers. In *Treatise on Geomorphology, vol. 9: Fluvial Geomorphology*, Shroder J, Wohl E (eds). Academic Press: San Diego, CA; 550–573.

Wohl W, David GCL. 2008. Consistency of scaling relations among bedrock and alluvial channels. *Journal of Geophysical Research: Earth Surface* **113**: F04013. https://doi.org/10.1029/2008JF000989.

Yager EM, Kirchner JW, Dietrich WE. 2007. Calculating bed load transport in steep boulder bed channels. *Water Resources Research* **43**: W07418. https://doi.org/10.1029/2006WR005432.

Zhang L, Parker G, Stark CP, Inoue T, Viparelli E, Fu X, Izumi N. 2015. Macro-roughness model of bedrock-alluvial river morphodynamics. *Earth Surface Dynamics* **3**: 113–138.

© 2019 John Wiley & Sons, Ltd. 